Available online at www.sciencedirect.com
SCIENCE DIRECT
Journal of Power Sources 149 (2005) 96–102
JOURNAL OF POWER SOURCES
www.elsevier.com/locate/jpowsour

A novel flow battery—A lead acid battery based on an electrolyte with soluble lead(II) III. The influence of conditions on battery performance

Derek Pletcher*, Richard Wills

School of Chemistry, The University, Southampton SO17 1BJ, England

Received 16 November 2004; received in revised form 24 January 2005; accepted 31 January 2005
Available online 17 March 2005

Abstract

The performance of an undivided flow battery based on the Pb(II)/Pb and PbO_2/Pb(II) couples in aqueous methanesulfonic acid as a function of state of charge, current density, electrolyte flow rate and temperature is reported. In addition, it is demonstrated that the cell chemistry can be rebalanced after multiple charge/discharge by allowing the excess lead metal deposited at the negative electrode to react with oxygen on open circuit.

Keywords: Flow batteries; Lead acid; Methanesulfonic acid

1. Introduction

In two recent papers [1,2], we reported preliminary studies of a flow battery based on the electrode reactions of lead(II) in methanesulfonic acid:

negative electrode

$$Pb^{2+} + 2e^- \underset{\text{discharge}}{\overset{\text{charge}}{\rightleftarrows}} Pb \quad (1)$$

positive electrode

$$Pb^{2+} + 2H_2O - 2e^- \underset{\text{discharge}}{\overset{\text{charge}}{\rightleftarrows}} PbO_2 + 4H^+ \quad (2)$$

overall battery reaction

$$2Pb^{2+} + 2H_2O \underset{\text{discharge}}{\overset{\text{charge}}{\rightleftarrows}} Pb + PbO_2 + 4H^+ \quad (3)$$

The system differs from the traditional lead acid battery [3,4] since lead(II) is highly soluble in methanesulfonic acid [5]. It also differs in concept and potential markets from the small box and button cell, secondary batteries based on soluble lead(II) that have been described in the patent literature [6–9] and a book chapter [10]. Moreover, these small batteries employed perchloric acid, fluorosilicic acid and/or tetrafluoroboric acid and methanesulfonic acid is both less hazardous and more materials friendly than these acids [5]. The proposed flow battery based on soluble lead(II) has potential advantages over all previously reported flow batteries, including Fe/Cr [11–13], V [14–18], Zn/Br_2 [19,20], polysulfide/Br_2 [21,22], since (a) it requires only a single electrolyte and can therefore employ simpler and cheaper cell configurations and also eliminates all costs and problems associated with a membrane and (b) the solution chemistry is straightforward.

In this paper, we discuss the influence of state of charge, current density, electrolyte flow rate and temperature on the flow battery characteristics. The electrolyte in the fully discharged battery was selected to be 1.5 M lead methanesulfonate and 0.9 M methanesulfonic acid. A

DOI of original article:10.1016/j.jpowsour.2005.01.049.
* Corresponding author. Tel.: +44 2380 593519; fax: +44 2380 593781.
E-mail address: dp1@soton.ac.uk (D. Pletcher).

0378-7753/$ – see front matter © 2005 Elsevier B.V. All rights reserved.
doi:10.1016/j.jpowsour.2005.01.048

high acid concentration is desirable for a low battery resistance while a high lead(II) concentration is essential both for a high storage density and a high rate of charge. It should be noted, however, that during charging, while the lead(II) concentration decreases, the acid concentration increases at twice the rate, see Eq. (3). The acid concentration in the initial electrolyte was chosen to be lower than might otherwise be considered optimum because of the wish for the lead(II) to be fully dissolved at all states of charge.

Another issue to be addressed is the chemical balance in the cell. It is critical to long term cycling that, on completion of a full charge/discharge cycle, the electrolyte composition and the electrodes return to their original state. In the proposed flow battery, the electrodes will only fulfil this requirement if the current efficiencies for lead deposition/dissolution and lead dioxide deposition/dissolution are exactly the same (and to minimise gas evolution, the current efficiencies should both be as close as possible to 100%). Even a small disparity in current efficiency between the positive and negative electrode chemistries will lead to build up of a solid on one of the electrodes during extensive cycling; a strategy to resolve this problem is essential.

2. Experimental

The experiments were carried out in a small undivided flow cell with two electrodes with geometric areas of 2 cm^2 and an interelectrode gap of 4 mm. Photographs of the cell and flow circuit are presented in Fig. 1. The cell along with the solution preparation and experimental procedures have been described in more detail in the earlier papers [1,2]. The electrodes consisted of a carbon powder/high density polyethylene composite back plate, thickness 3.2 mm, with an active layer on the surface produced by heat bonding under pressure. Three types of electrodes with different active layers were used:

(i) type 1 electrodes were fabricated by pressing a piece of 40 ppi nickel foam, initial thickness 1.8 mm into the plate with a pressure of 6 kg cm^{-2} at 433 K;
(ii) type 2 electrodes were fabricated by pressing a piece of 70 ppi reticulated vitreous carbon, initial thickness 1.5 mm into the plate in the same conditions;
(iii) type 3 electrodes were prepared from type 2 by scraping away the reticulated carbon layer with a knife. This leaves a rough surface with many vitreous carbon particles.

SEM photographs of these structures have previously been reported [2]. Unless otherwise stated, experiments in this paper employed type 1 as the negative electrodes and type 3 as the positive electrode.

Fig. 1. Photographs showing (A) flow cell components and (B) assembled flow cell system. (1) Cell clamp; (2) flow compartment plates; (3) gasket and interelectrode spacer; (4 and 5) electrodes; (6) assembled flow cell; (7) peristaltic pump and pump head; (8) pump controller; (9) potentiostat/galvanostat; (10) electrolyte reservoir; (11) thermostated water bath.

3. Results and discussion

3.1. State of charge

The influence of state of charge was investigated by carrying out experiments with five electrolyte compositions that assumed that the electrolyte in the fully uncharged state was 1.5 M lead methanesulfonate and 0.9 M methanesulfonic acid and that the charge reaction follows the stoichiometry described by Eq. (3).

Fig. 2 reports current density versus cell voltage characteristics for a charged cell with the five electrolyte compositions. These were obtained by charging the cell for 1 h at 20 mA cm^{-2} in 1.5 M lead methanesulfonate and 0.9 M methanesulfonic acid before the cell was drained and filled with the electrolyte composition to be studied. The cell charge characteristic was then obtained by ramping the current density from 0 to 100 mA cm^{-2} at 0.5 mA cm^{-2} s^{-1} while monitoring the cell voltage. The cell discharge characteristic was recorded in the same way with the direction of current flow reversed. In Fig. 2, it can be seen that the open circuit potential for the cell shifts significantly higher as the experiment is commenced with a low lead(II), high proton concentration electrolyte equivalent to a more charged battery. This is to be expected based on the Nernst equation for a cell with the chemistry of Eq. (3) (the lead(II) concentration decreases and

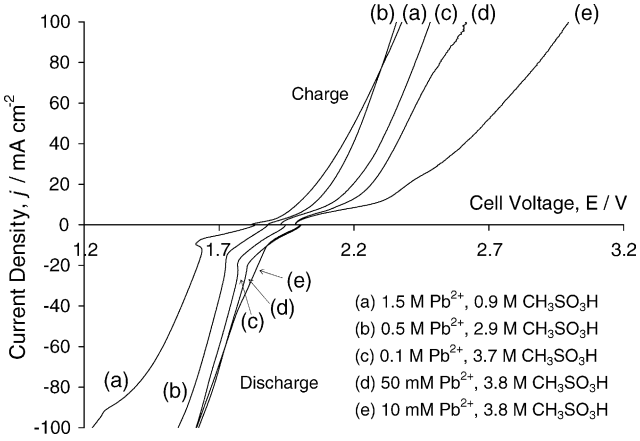

Fig. 2. Current density vs. cell voltage characteristics as a function of electrolyte composition (i.e. state of charge). Cell with reticulated vitreous carbon positive electrode and Ni foam negative electrode charged for 1 h at 20 mA cm^{-2} in 1.5 M lead methanesulfonate and 0.9 M methanesulfonic acid before the electrolyte was changed to that shown. Curves recorded by ramping current at 0.5 mA cm^{-2} s^{-1} from the open circuit potential. Temperature 298 K; electrolyte flow rate 9.9 cm s^{-1}.

the proton concentration increases as the battery is charged)

$$E_{\text{open circuit}} = E^{\circ}_{PbO_2/Pb^{2+}} - E^{\circ}_{Pb^{2+}/Pb} - \frac{2.3RT}{F}\log c_{Pb^{2+}} + \frac{4.6RT}{F}\log c_{H^+} \quad (4)$$

where $E^{\circ}_{PbO_2/Pb^{2+}}$ and $E^{\circ}_{Pb^{2+}/Pb}$ are the formal potentials for the two couples and it is assumed that the solid phases and water are in their standard states. Some change in cell voltage with state of charge is an inevitable characteristic of the proposed battery. On the other hand, this change in open circuit potential does not influence the energy storage efficiency for the cell. It is the overpotentials associated with the two electrode reactions and the IR drop through the cell (along with the current efficiencies) that determine the energy efficiency. The IR drop through the electrolyte is readily calculated using the conductivities reported previously [1] and it reaches ~100 mV when the current density is 100 mA cm^{-2}; the IR drop in the electrodes is negligible in comparison. Hence, a substantial fraction of the deviations from the open circuit potentials shown in the responses of Fig. 2 result from the overpotentials associated with the electrode reactions, particularly the deposition and dissolution of the lead dioxide [1]. The overpotentials increase steadily with cell current density during both charge and discharge. On discharge, there are only relatively small differences between the overpotentials and this is to be expected since there are no mass transport limitations associated with the electrode reactions. During discharge, the overpotentials are higher in the "high" lead, "low" proton concentration electrolyte, solution (a), and this may result from a consequent larger swing in the proton concentration within the pores of the lead dioxide solid as it is reduced (again, see Eq. (4)). On charge, the response for solution (e), the 10 mM Pb^{2+} solution shows a rapid increase in

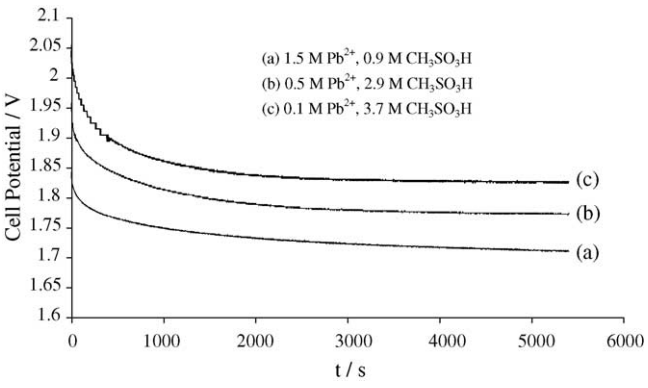

Fig. 3. Open circuit cell voltage as a function of time after the battery was charged for 1 h at 20 mA cm^{-2} with three electrolyte compositions representing different states of charge.

cell voltage with current density to a high value; it is probable that oxygen and hydrogen evolution occur due to an insufficient flux of lead ions to the two electrodes. Certainly, gas bubbles are observed in the reservoir. With solution (d) containing 50 mM Pb^{2+} a similar tendency is evident but only at the highest current densities. Otherwise for solutions (a)–(c) the characteristics are similar and no gas bubbles are seen. At least on the timescale of these experiments, i.e. 200 s, it would appear that the cell can be charged at least until the lead(II) concentration has dropped to below 0.1 M.

The influence of state of charge on battery performance was further investigated by carrying out charge/discharge cycling in electrolytes with appropriate compositions; these experiments were commenced with uncharged electrodes. The results are reported in Table 1. Again, the open circuit potentials were observed to shift positive with increasing acid and decreasing lead(II) concentrations. In this table, the open circuit potentials are significantly less positive than those that would be read from Fig. 2 and this is because the cell was allowed to reach a steady state before the potential was recorded. After the end of the charge period, the cell was allowed to sit on open circuit while the cell voltage was monitored, see Fig. 3. The cell voltage was found to decrease markedly and only reached a steady value after an extended period. A likely explanation is that the acid and lead(II) concentrations within the pores of the lead dioxide deposit during charge are markedly different from those in the bulk electrolyte, see Eq. (3), and relaxation to the bulk value requires diffusion and this is a slow process. Consistent with this explanation, it can be seen in Fig. 3 that the drift in cell voltage is greatest for the most dilute Pb^{2+} solution. Another possibility is that some self discharge occurs at the outer surfaces of the lead dioxide leading to an insoluble lead(II) product, see later; self discharge of traditional lead dioxide batteries is a common phenomenon and when used for reserve supplies and similar applications they are always trickle charged [4,19,23]. With the soluble lead battery, however, there was no loss in charge efficiency if the battery was stood on open circuit for 1 h between charge and discharge. Table 1 also reports the

Table 1
Battery performance data with three initial electrolyte compositions (lead methanesulfonate + methanesulfonic acid)

Initial electrolyte composition (M)		Open circuit battery voltage after charge (V)	Charge efficiency (%)	Energy efficiency (%)
Pb^{2+}	H^+			
1.5	0.9	1.71	93	76
0.5	2.9	1.78	86	72
0.1	3.7	1.83	63	54

The flow cell was charged at 20 mA cm^{-2} for 900 s and then discharged at the same rate until the cell voltage dropped to 1.2 V. Temperature 298 K; electrolyte flow rate 9.9 cm s^{-1}.

charge and energy efficiencies for the sixth charge/discharge cycle for the cell with each electrolyte when the data have reached a steady state. Clearly, the cell performs well over a wide range of lead(II) concentrations but there is a decline in performance when the electrolyte contains <0.1 M lead(II).

3.2. Rate of charge/discharge

Fig. 2 is one representation of the influence of current density on both charge and discharge. With sufficient lead(II) in the electrolyte, it is to be expected that the charge and discharge are both efficient reactions but an increase in current density is at a cost of increased overpotentials and a loss in energy efficiency.

This was confirmed by a series of charge/discharge cycle experiments at current densities of 20, 40 and 60 mA cm^{-2} with the electrolyte, 1.5 M lead methanesulfonate and 0.9 M methanesulfonic acid. The cell voltage versus time characteristics are shown in Fig. 4 (see also Fig. 7 in [2]). The responses are very similar in form and the charge efficiency is always ~90%. The overpotentials on both charge and discharge, however, increase with current density and hence the energy efficiency decays with increased current density.

The responses also show that the behaviour during the first charge is different from that in subsequent cycles. The cell voltage during the first charge is constant at a rather high value. In subsequent cycles, the cell voltage starts at a significantly lower value but rises over a period to the value during the first charge. Such behaviour has been noted previously [1,2] and demonstrated to be associated with the positive electrode. This phenomenon was investigated further. Using a vitreous carbon RDE in a solution consisting of 1.5 M lead methanesulfonate and 0.9 M methanesulfonic acid, lead dioxide was deposited at 10 mA cm^{-2} for 600 s and then discharged at 100 mA cm^{-2} before the disc was washed and examined. By eye, the charged electrode is clearly covered by a thick layer of black oxide and after discharge it had largely returned to the appearance of vitreous carbon although there were small patches of deposit appearing to be a much thinner film. Fig. 5(b) reports a scanning electron micrograph of one such patch and in Fig. 5(a) the lead dioxide before reduction is also shown. Before discharge, there is a uniform layer of lead dioxide on the vitreous carbon. After the discharge step, most of the deposit has dissolved (as confirmed by SEM at lower magnification) but some poorly conducting

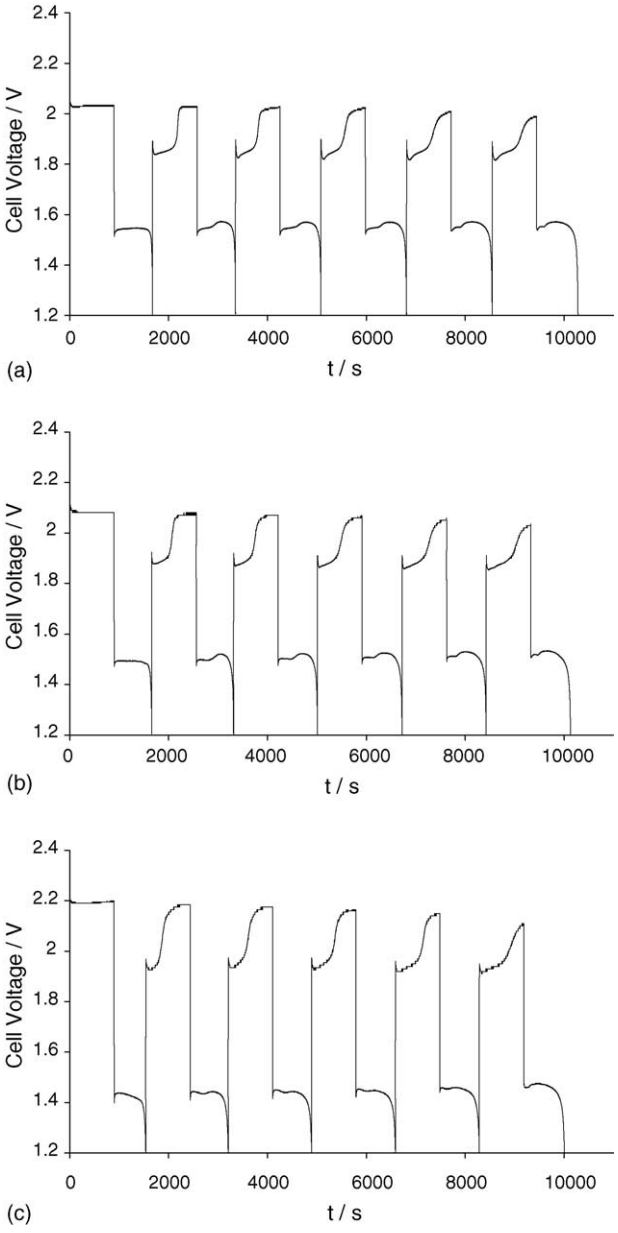

Fig. 4. Cell voltage vs. time responses for six charge/discharge cycles at current densities of (a) 20 mA cm^{-2}; (b) 40 mA cm^{-2}; (c) 60 mA cm^{-2}. Electrolyte: 1.5 M lead methanesulfonate and 0.9 M methanesulfonic acid. Temperature 298 K; electrolyte flow rate 9.9 cm s^{-1}.

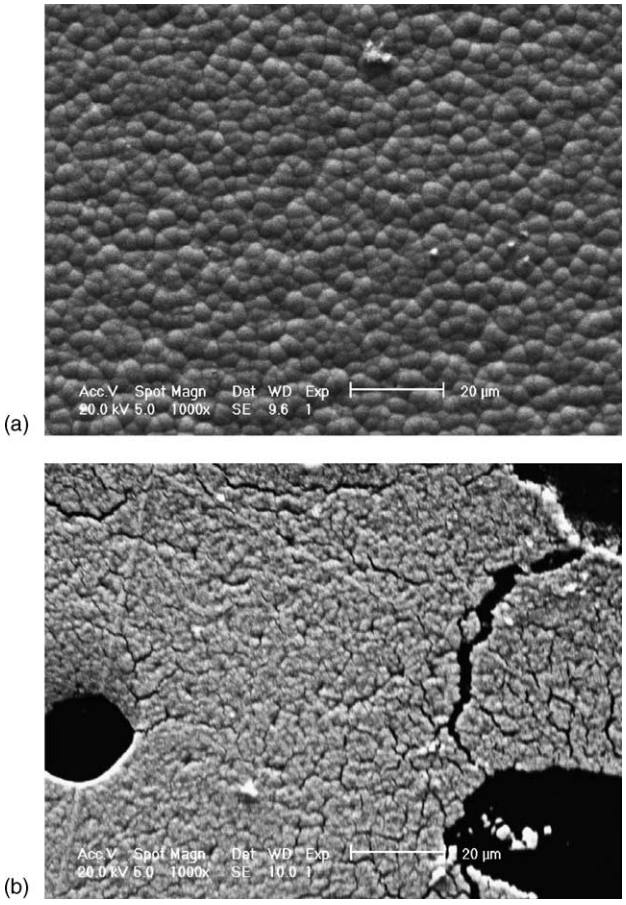

Fig. 5. Scanning electron micrographs of (a) the PbO_2 layer deposited on a vitreous carbon RDE at 10 mA cm^{-2} for 600 s and (b) the deposit remaining after dissolution of this layer at 100 mA cm^{-2}. Electrolyte: 1.5 M lead methanesulfonate + 0.9 M methanesulfonic acid. Temperature 298 K.

solid clearly remains in patches on the carbon surface. It is, however, only a small fraction of the PbO_2 deposited and the rapid discharge was selected to maximise the insoluble material formed. Moreover, it clearly has a different structure to the PbO_2 while EDAX analysis of the deposit shows that the ratio of oxygen:lead is close to half that found for the PbO_2 suggesting that the deposit is PbO. This lead(II) oxide could arise during the dissolution of the PbO_2 if the concentration of Pb^{2+} in the boundary layer close to the electrode becomes high enough to exceed the solubility product of a lead(II) species. The proton concentration in this boundary layer could also become depleted, aiding deposition of the lead species. Effectively, there are two reduction routes leading to soluble and insoluble lead(II) and the ratio of the two products will depend on the dissolution conditions, e.g. current density, temperature. It is probable that this deposit is reoxidised back to PbO_2 more readily than the Pb^{2+} in solution and this is the cause of the low cell voltage during the early stages of charge in second and subsequent cycles. We would, however, emphasise that we have seen no evidence to suggest that this deposit degrades the cell performance and it can be regarded as a bonus since it leads to a better energy efficiency.

Table 2
Battery performance as a function of discharge current density

Discharge current density (mA cm^{-2})	Discharge voltage (V)	Charge efficiency (%)	Energy efficiency (%)
20	1.56	85	66
40	1.48	78	59
60	1.43	77	58
80	1.33	65	42
100	1.26	62	44

The battery was charged at 20 mA cm^{-2} for 1 h and then discharged at various current densities. Electrolyte: 1.5 M lead methanesulfonate and 0.9 M methanesulfonic acid. Temperature 298 K; electrolyte flow rate 9.9 cm s^{-1}.

While the form of the lead and lead dioxide deposits and the current efficiency for their formation would be expected to be a strong function of the current density during charge (and loose deposits were always observed at current densities of 40 mA cm^{-2} and above), it is to be expected that the current density during discharge would have less influence on cell performance. To test this hypothesis, a series of experiments were carried out where the cell was charged in 1.5 M lead methanesulfonate and 0.9 M methanesulfonic acid at 20 mA cm^{-2} for 1 h and then discharged at different rates. The results are reported in Table 2. Indeed, up to 60 mA cm^{-2}, the charge efficiency only decreases slightly but there is a drop in the cell voltage and this leads to some degradation in the energy efficiency. At 100 mA cm^{-2}, even the charge efficiency is severely diminished.

3.3. Electrolyte flow rate and electrode structure

Charge/discharge cycling experiments with the cell containing 1.5 M lead methanesulfonate and 0.9 M methanesulfonic acid, and using a current density of 20 mA cm^{-2} showed no dependence of the behaviour on flow rate over the range 1–10 cm s^{-1}. However, mass transport is not likely to be a factor in these conditions. Rather mass transport will be important at high charge rates and will grow in importance as the lead(II) in solution is consumed. In reality, with the electrodes employed, using measurements of limiting current densities, it is not possible to simply distinguish the influence of the electrode structures on the mass transport coefficient from differences in the real surface areas of the materials. For three-dimensional electrodes, the limiting current density, j_L, is given by

$$j_L = nFk_m A_e V_e c \quad (5)$$

where k_m is the mass transfer coefficient, A_e the specific surface area, V_e the volume of the electrode, n the number of electrons transferred/molecule of reactant, F the Faraday constant and c is the concentration of reactant.

Fig. 6 shows plots of $\log j_L$ versus $\log v$ for the uncovered back plate and both types 2 and 3 electrodes in a solution

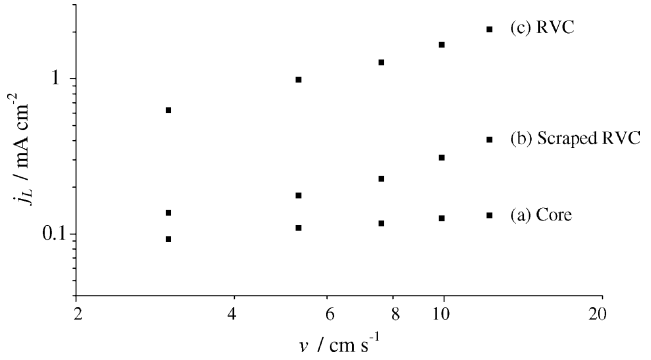

Fig. 6. Limiting current density as a function of the mean linear flow rate of the electrolyte vs. cell with (a) a flat plate carbon electrode; (b) a scraped reticulated vitreous carbon electrode; (c) a reticulated vitreous carbon electrode. Data for the oxidation of ferrocyanide. Solution: 10^{-3} M $K_4Fe(CN)_6 + 10^{-2}$ M $K_3Fe(CN)_6$. Temperature 298 K.

containing 1 mM ferrocyanide and 10 mM ferricyanide; the limiting current densities are based on the geometric area of the back plate (2 cm^2) and v is the mean linear flow rate of the electrolyte. Using the smooth back plate as the electrode the current densities are of the order of 0.1 mA cm^{-2} (equivalent to a mass transfer coefficient of 10^{-3} cm s^{-1}) and there is a small increase with increase in the flow rate over the range 1–15 $\times$ 10^{-3} cm s^{-1}. With the very rough surface of type 3 electrodes, the current densities increase by a factor up to three and the dependence on flow rate increases; these result from the turbulence introduced by the vitreous carbon fragments. With the type 2 electrodes, the current densities are >10 higher then at the flat plate and this arises from enhancements in both mass transfer coefficient and electrode surface area. The values of k_mA_e range between 0.08 and 0.3 s^{-1} with the flow rate range investigated. This is similar to values reported earlier [24,25] and shows one clear advantage for the three-dimensional electrode. The limiting current density at the reticulated vitreous carbon (type 2) and a flow rate of 10 cm s^{-1} for a 0.1 M lead(II) solution may be estimated as >200 mA cm^{-2} confirming the advantage of these conditions if the battery were to be charged to low lead concentrations. It may be noted that depletion of the electrolyte initially containing 1. 5 M Pb^{2+} to a lead concentration of 0.1 M would give an energy storage capability of ~60 Wh/l of the electrolyte. Another advantage of the three-dimensional electrode is that the Pb and PbO_2 deposits on the electrodes will be formed at a lower local current density and it is to be expected the deposits will then show greater uniformity and better adhesion [26].

3.4. Temperature

Charge/discharge cycling experiments were carried out at five temperatures within the range 273–333 K using the electrolyte, 1.5 M lead methanesulfonate and 0.9 M methanesulfonic acid and a cycle regime of charging at 20 mA cm^{-2} for 900 s followed by discharge at the same current density until the cell voltage dropped to 1.2 V. Data taken from the sixth cycle are reported in Table 3. With increasing temperature, there is a substantial decrease in the overpotential during charge and a small decrease in the overpotential during discharge. Over the range 273–313 K, there is little change in charge efficiency. At higher temperatures, the charge efficiency decreases and this may result from the formation of some soluble lead(IV) species at the higher temperature.

Table 3
Battery performance as a function of temperature

T (K)	Battery voltage (V)		Charge efficiency (%)	Energy efficiency (%)
	Charge	Discharge		
273	2.04	1.54	91	72
298	2.01	1.54	93	76
313	1.95	1.56	90	74
323	1.89	1.57	77	67
333	1.84	1.57	67	59

Data from sixth charge/discharge cycle. Current density for charge and discharge: 20 mA cm^{-2}. 900 s charge. Electrolyte: 1.5 M lead methanesulfonate and 0.9 M methanesulfonic acid. Electrolyte flow rate 9.9 cm s^{-1}.

Overall, 273–313 K seems to be the preferable temperature range for operation of the battery.

3.5. Balancing the cell chemistry

When cells were fully discharged and dismantled after extensive cycling, some lead metal could be seen remaining on the negative electrode. This suggests that the current efficiencies of the reactions at the negative electrode are higher than those at the positive electrode and the likely reason is the evolution of some oxygen in parallel to lead dioxide deposition. Indeed, in the light of experience of the charge balances during cyclic voltammetry of lead and lead dioxide deposition and related experiments, the build up of lead on the negative electrode is surprisingly slow. Even so, a strategy for rebalancing the cell chemistry is essential to prevent continuous build up of the lead on the negative electrode.

One approach is to periodically dissolve the lead back into solution using a non-electrochemical procedure that does not require the irreversible addition of chemicals into the electrolyte. Oxygen is a potential oxidant when dissolution should occur by the reaction.

$$2Pb + 4H^+ + O_2 \rightarrow 2Pb^{2+} + 2H_2O \quad (6)$$

Excess oxygen should then be readily removed after the completion of the dissolution.

In order to demonstrate that lead metal corrodes in a facile way in the battery electrolyte and to estimate the rate of dissolution, the following experiment was carried out. The cell was charged at a current density of 40 mA cm^{-2} for 1800 s using the electrolyte, 1.5 M lead methanesulfonate and 0.9 M methanesulfonic acid. After charging, the cell was drained and washed before the positive electrode was removed and replaced by a polymer sheet (in order to ensure that any Pb(II)

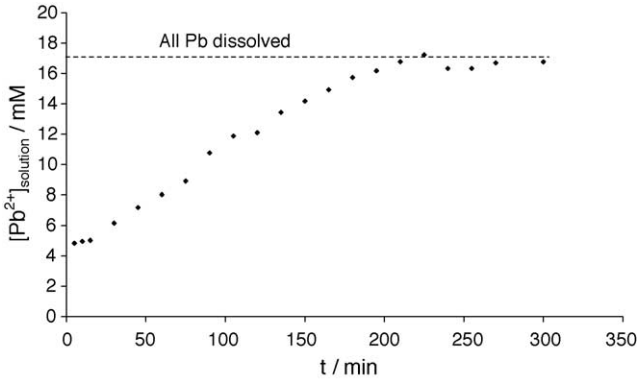

Fig. 7. Concentration of lead(II) in solution as a function of time when flowing O_2 saturated 0.9 M methanesulfonic acid through the cell on open circuit after the removal of the positive electrode. The lead was deposited with a current density of 40 mA cm^{-2} for 1800 s. Temperature 298 K; electrolyte flow rate 9.9 cm s^{-1}.

subsequently found in solution came from the dissolution of lead, not lead dioxide). Then, oxygen saturated methanesulfonic acid (0.9 M) was flowed through the cell and concentration of lead(II) in the acid was monitored as a function of time using a vitreous carbon rotating disc electrode (also reference and counter electrodes) in the reservoir and a calibration plot of limiting current versus lead(II) concentration. The results are shown in Fig. 7 where it can be seen that the lead(II) in solution increases linearly with time and that all the lead corrodes into solution over a period of 230 min. It is not to be expected that the high lead(II) concentration present in the battery electrolyte will slow down the dissolution; the lead(II) free initial acid was used in order to aid the facile analysis of the lead(II) accumulating in the electrolyte during dissolution. It is, of course, probable that the rate of dissolution could be enhanced by increasing the temperature or supply of oxygen.

4. Conclusions

The soluble lead(II), lead–acid flow battery has been shown to give a good performance over a range of conditions including state of charge, current density, electrolyte flow rate and temperature. It has also been shown that although lead builds up on the negative electrode during extended cycling, it may be removed by exposing the electrode to an oxygen containing battery electrolyte after a full discharge of the battery.

Acknowledgements

The authors would like to thank Regenesys Technologies Ltd. for financial support of the work and Dr. Jon Cox of Regenesys Technologies Ltd. for the fabrication of the electrodes.

References

[1] A. Hazza, D. Pletcher, R. Wills, Phys. Chem. Chem. Phys. 6 (2004) 1773.
[2] D. Pletcher, R. Wills, Phys. Chem. Chem. Phys. 6 (2004) 1779.
[3] D. Linden (Ed.), Handbook of Batteries, McGraw Hill, 1994.
[4] H. Bode, Lead–Acid Batteries, John Wiley, 1977.
[5] M.D. Gernon, M. Wu, T. Buszta, P. Janney, Green Chem. 1 (1999) 127.
[6] F. Beck, US Patent 4,001,037 (1977).
[7] R. Wurmb, F. Beck, K. Boehlke, US Patent 4,092,463 (1978).
[8] P.O. Henk, Z.A.A. Piontkowski, US Patent 4,331,744 (1982).
[9] P.O. Henk, US Patent 4,400,449 (1983).
[10] F. Beck, in: A.T. Kuhn (Ed.), The Electrochemistry of Lead, Academic Press, New York, 1979, p. 65.
[11] F. Beck, P. Ruetschi, Electrochim. Acta 45 (2000) 2467.
[12] K. Nozaki, T. Ozawa, Prog. Batteries Sol. Cells 5 (1984) 327.
[13] M. Bartolozzi, J. Power Sources 27 (1989) 219.
[14] M. Kazacos, M. Skyllas-Kazacos, J. Electrochem. Soc. 136 (1989) 2759.
[15] M. Skyllas-Kazacos, D. Kasherman, R.R. Hong, M. Kazacos, J. Power Sources 35 (1991) 399.
[16] C. Menictas, D.R. Hong, Z.H. Yan, J. Wilson, M. Kazacos, M. Skyllas-Kazacos, Proceedings of the Electrical Engineering Congress, Sydney, November 1994.
[17] Reviews available at http://www.ceic.unsw.edu.au/centers/vrb/webframe/option1.htm.
[18] I. Takefumi, K. Takashi, I. Atsuo, K. Kouhei, T. Hara, T. Nobuyuki, Proceedings of the Society of Automotive Engineers, 1999, 1999-01-2616.
[19] P.C. Butler, P.A. Eidler, P.C. Grimes, S.E. Klassen, R.C. Miles, in: D. Linden (Ed.), Handbook of Batteries, McGraw Hill, 1994 (Chapter 37).
[20] P. Lex, B. Jonshagen, Power Eng. J. 13 (1999) 142.
[21] A. Price, S. Bartley, S. Male, G. Cooley, Power Eng. J. 13 (1999) 122.
[22] S. Male, Proceedings of the 13th International Forum on Electrolysis in the Chemical Industry, Clearwater Beach, FL, November 1999.
[23] M. Barak (Ed.), Electrochemical Power Sources: Primary and Secondary Batteries, Peregrinus, 1980.
[24] D. Pletcher, F.C. Walsh, in: J.D. Genders, N.L. Weinberg (Eds.), Electrochemical Technology for a Cleaner Environment, The Electrosynthesis Co., Lancaster, NY, 1992.
[25] J.M. Friedrich, C. Ponce-de-Leon, G.W. Reade, F.C. Walsh, J. Electroanal. Chem. 561 (2004) 203.
[26] D. Pletcher, R. Wills, following paper.